Journal of the Mechanical Behavior of Biomedical Materials 84 (2018) 273–280

Contents lists available at ScienceDirect

Journal of the Mechanical Behavior of Biomedical Materials

journal homepage: www.elsevier.com/locate/jmbbm

A comparative analysis of the avian skull: Woodpeckers and chickens

Jae-Young Jung[a,*], Andrei Pissarenko[b], Nicholas A. Yaraghi[c], Steven E. Naleway[d], David Kisailus[c,e], Marc A. Meyers[a,b,f], Joanna McKittrick[a,b]

[a] Materials Science and Engineering Program, University of California, San Diego, La Jolla, CA 92093, USA
[b] Department of Mechanical and Aerospace Engineering, University of California, San Diego, La Jolla, CA 92093, USA
[c] Materials Science and Engineering Program, University of California, Riverside, CA 92521, USA
[d] Department of Mechanical Engineering, University of Utah, Salt Lake City, UT 84112, USA
[e] Department of Chemical and Environmental Engineering, University of California, Riverside, CA 92521, USA
[f] Department of NanoEngineering, University of California, San Diego, La Jolla, CA 92093, USA

ARTICLE INFO

Keywords:
Woodpecker
Chicken
Skull bone
X-ray micro-computed tomography
Scanning electron microscopy
Nanoindentation

ABSTRACT

Woodpeckers peck at trees without any reported brain injury despite undergoing high impact loads. Amongst the adaptations allowing this is a highly functionalized impact-absorption system consisting of the head, beak, tongue and hyoid bone. This study aims to examine the anatomical structure, composition, and mechanical properties of the skull to determine its potential role in energy absorption and dissipation. An acorn woodpecker and a domestic chicken are compared through micro-computed tomography to analyze and compare two- and three-dimensional bone morphometry. Optical and scanning electron microscopy with energy dispersive X-ray spectroscopy are used to identify the structural and chemical components. Nanoindentation reveals mechanical properties along the transverse cross-section, normal to the direction of impact. Results show two different strategies: the skull bone of the woodpecker shows a relatively small but uniform level of closed porosity, a higher degree of mineralization, and a higher cortical to skull bone ratio. Conversely, the chicken skull bone shows a wide range of both open and closed porosity (volume fraction), a lower degree of mineralization, and a lower cortical to skull bone ratio. This structural difference affects the mechanical properties: the skull bones of woodpeckers are slightly stiffer than those of chickens. Furthermore, the Young's modulus of the woodpecker frontal bone is significantly higher than that of the parietal bone. These new findings may be useful to potential engineered design applications, as well as future work to understand how woodpeckers avoid brain injury.

1. Introduction

Woodpeckers use their beaks as a hammering tool without sustaining any reported traumatic brain injury or concussion during pecking (May et al., 1976, 1979). The hammering rates are up to 20 Hz with impact speeds ranging from 1 to 7 m/s, and deceleration up to 1200 ***g*** (May et al., 1979). There have been several attempts to reveal the key elements of the successful utilization of their beaks and heads as excavating tools. It has been pointed out that woodpeckers have strong neck muscles (May et al., 1976), zygodactyl feet (two toes pointing forwards and two pointing backwards) (May et al., 1979; Bock and Miller, 1959), a large portion of spongy bone on the skull with relatively little cerebrospinal fluid (May et al., 1976), and the hyoid apparatus and its internal bone (hyoid bone) (Bock, 1999; Oda et al., 2006; Zhou et al., 2009; Wang et al., 2011a; Yoon and Park, 2011; Liu et al., 2015), identified as a highly-elongated and unusual structure only found in woodpeckers and hummingbirds. In contrast, chickens do not hammer against trees to sustain their diet; they use their upper and lower beaks to pick up food from the ground (Lee et al., 2014), and possess a short hyoid apparatus (Homberger and Meyers, 1989). A study conducted by Mehdizadeh et al. (2015) evaluated the biomechanics of the head and beak motion of broiler chickens (*Gallus gallus domesticus*) during feeding; an image analysis was used to identify head's movement and concluded that chickens do not peck against the ground or other heavy objects in the way that woodpeckers do. Given these diverging pecking habits, a comparative study of the heads of woodpeckers and chickens can be an insightful approach towards identifying the anatomical features that provide woodpecker's remarkable resistance to dynamic impacts.

To better explain the concept of energy dissipation in the woodpecker's head during hammering, the head's anatomy and mechanical properties need to be understood in detail. Lee et al. (2014) reported a reduced elastic modulus of 8.7 GPa for the lower rhamphotheca (a keratinized outer sheath mainly composed of β-keratin (Wang et al.,

* Correspondence to: 9500 Gilman Dr. MC 0418, La Jolla, CA 92093-0418, USA.
E-mail addresses: jyjung@ucsd.edu (J.-Y. Jung), jmckittrick@eng.ucsd.edu (J. McKittrick).

https://doi.org/10.1016/j.jmbbm.2018.05.001
Received 30 October 2017; Received in revised form 1 April 2018; Accepted 1 May 2018
Available online 02 May 2018
1751-6161/ Published by Elsevier Ltd.

2016)) of a red-bellied woodpecker (*Melanerpes carolinus*) obtained from nanoindentation tests. Wang et al. (2011a) reported, using a 3D finite element analysis, that woodpeckers have a longer lower beak bone (1.2 mm difference) than the upper one, so that the first impact occurs at the lower beak bone. Zhu et al. (2014) reported that the Young's moduli in the skull showed a lower value (4 ~ 9 GPa) than those of beak bones (~ 30 GPa (Lee et al., 2014)). The aforementioned datasets of the woodpecker skull bones are valuable resources to investigate and mimic the impact-resistant structures/materials found in nature and can be used as a template for a biomimic approach to develop new materials. However, the previous data were collected from only two species (i.e., a red-bellied woodpecker and a great-spotted woodpecker), and showed a broad range of the Young's moduli from 0.31 GPa (Wang et al., 2011a, 2011b; Wang and Fan, 2013) to 6.6 GPa (Wu et al., 2015). Another dataset from a different species (an acorn woodpecker in this manuscript) can be a valuable addition to the field of biomechanics. Other factors, such as chemical composition, degree of mineralization or calcification and porosity, have not been discussed in detail. Such variations in terms of mechanical properties highlight the necessity to expand our knowledge of the woodpecker's head anatomical features at different length scales. The head of a chicken provides a good reference to study the woodpecker head, the anatomy of the head of chickens has been well studied; there are many sources of scientific papers about its anatomy (Jollie, 1957; Van Den Heuvel, 1991) and open-source electronic 2D/3D imaging data (http://digimorph.org/). In addition, the biomechanics of the pecking behavior of the chicken has been well studied (Mehdizadeh et al., 2015; Tolman, 1967; Van Den Heuvel and Berkhoudt, 1997) compared to other birds. In order to find food, both species peck, but against the different substrates (i.e., trees vs. dirt on ground), implying their structural designs and materials can be altered. This biomechanical data is useful to our biomechanics approach as it provides a direct comparison with respect to the shape of the bills, the structural components of the head, and pecking motion. Finally, the microstructural features and chemical composition of the chicken skeleton can be found in the literature. Structural properties of the beak bone has been reported by Lee et al. (2014), who determined that the chicken beak bone had a porosity of ~42%, while the beak bone of woodpeckers had a porosity of ~10%, which is comparable to other structural biological materials, such as non-mineralized materials (i.e., a 3% of porosity in horse hoof and a 6% in rhino horn) and mineralized materials (i.e., a 5% of porosity in compact bovine femur bone and a 12% in human dentin) (McKittrick et al., 2010). Thus, chickens provide a reasonable control based on extensive microstructural data, biomechanical analyses of their pecking habits, and material characterization data of the head.

We hypothesize that the differences in pecking behavior can be seen in the anatomy and mechanics of these two species. To confirm the proposed hypothesis, this study aims to identify the anatomical structure, as well as the mechanical/chemical properties of woodpecker skull bones. As a control group of non-pecking avian species, a domestic chicken was chosen and compared to highlight anatomical differences with woodpeckers. Characterization of mechanical and chemical properties of the skull bone for both species intends to further define the structure-properties relationships in avian bones and the effects that pecking behavior has on these relationships.

2. Materials and methods

2.1. Sample collection and preparation

This study was conducted under the approval of an animal care and use program by the Institutional Animal Care and Use Committee (IACUC) at the University of California, San Diego (Tissue Permit Number: T14068).

An adult acorn woodpecker (*Melanerpes formicivorus*) was donated after death from a Northern California ranch. The bird was immediately frozen in a freezer at −20 °C, and kept as such during transport to the lab. The woodpecker specimen, stored at −20 °C, was gradually thawed at room temperature for 30 min prior to testing. All tests were performed under ambient conditions (25 °C, 60% relative humidity). Additionally, a dried chicken skull (*Gallus gallus*), prepared for taxidermy purposes (using *Dermestidae*, known as flesh eating beetles) without whitening and de-greasing (Marbury, 2014), was purchased from an online vendor (Atlantic Coral Enterprise, Inc.). There were no chemical and heat treatments on the sample prior to our study.

2.2. Micro-computed tomography (μ-CT)

The acorn woodpecker was scanned by μ-CT (SkyScan 1076, Bruker microCT, Kontich, Belgium) with a rotation step of 0.7°, a 100 kV acceleration voltage, and an isotropic voxel size of 9.06 μm. Raw data of a domestic chicken were obtained from digimorph.org (http://digimorph.org/), operated by the High-Resolution X-ray CT Facility at the University of Texas, Austin. The chicken skull was scanned at 200 kV with an isotropic voxel size of 77.6 μm. Each skull bone was visualized and analyzed using Amira software (FEI Visualization Sciences Group, Burlington, MA) for visualization and a 3D rendering with mineral density color scaling.

μ-CT scans of the chicken and woodpecker were analyzed to compare the average thicknesses of cortical (T_c) and trabecular (T_b) bones. ImageJ software (National Institutes of Health, Bethesda, MD) and its open source plugin, BoneJ (Doube et al., 2010), were used for 2D bone morphometric analysis.

CTan software (Bruker MicroCT, Kontich, Belgium) was used for 2D and 3D bone morphometric analysis to select the range of the start and end slices based on the 3D image to include only the skull bone part. A series of binarized images with a certain range of threshold values was reconstructed and saved prior to the bone morphometric analysis (Bouxsein et al., 2010). The segmented images corresponding to the skull region were isolated to estimate the total volume of the skull bone (V_s) and brain (V_b), the whole head volume ($V_w = V_s + V_b$), the ratio of the skull bone volume to the whole head volume (V_s/V_w), and the ratio of the average cortical thickness to the whole head volume (T_c/V_w). For a simplified comparative analysis, the effects of other soft tissues, such as muscles, cerebrospinal fluids, and eyes, were not considered in this analysis.

To calculate porosity in a specific volume of interest (VOI), the standardized terminology was adapted from the American Society for Bone and Mineral Research for bone histomorphometry (Parfitt et al., 1987). Specifically, the tissue volume (TV) is defined as the volume of selected VOI, and is the sum of the bone tissue (bone volume) and void volume area (pores) (Parfitt et al., 1987). The bone volume (BV) is defined as the volume of binarized objects within the VOI, where is a bright contrast region of the bone tissue (Parfitt et al., 1987). The ratio of the bone volume to tissue volume (BV/TV) is derived from above two definitions. Then, the closed, open, and total porosities were calculated in the same VOI. Here, a closed pore in 3D is defined as a connected assemblage of space (black) voxels that is fully surrounded on all sides in 3D by solid (white) voxels in a segmented binary image, while an open pore is defined as any space located within a solid object or between solid objects, which has any connection in 3D to the space outside the object (Bouxsein et al., 2010; Parfitt et al., 1987; Meyers et al., 2013; Odgaard and Gundersen, 1993). A benefit of binarized 3D image morphometric analysis is that the software successfully recognized the closed and open cells, unlike the 2D image analysis, which cannot distinguish between closed and open cells because of limited geometrical information.

2.3. Microstructure and chemical composition

The chicken and woodpecker skulls were analyzed by scanning electron microscopy (SEM) and X-ray energy dispersive spectroscopy

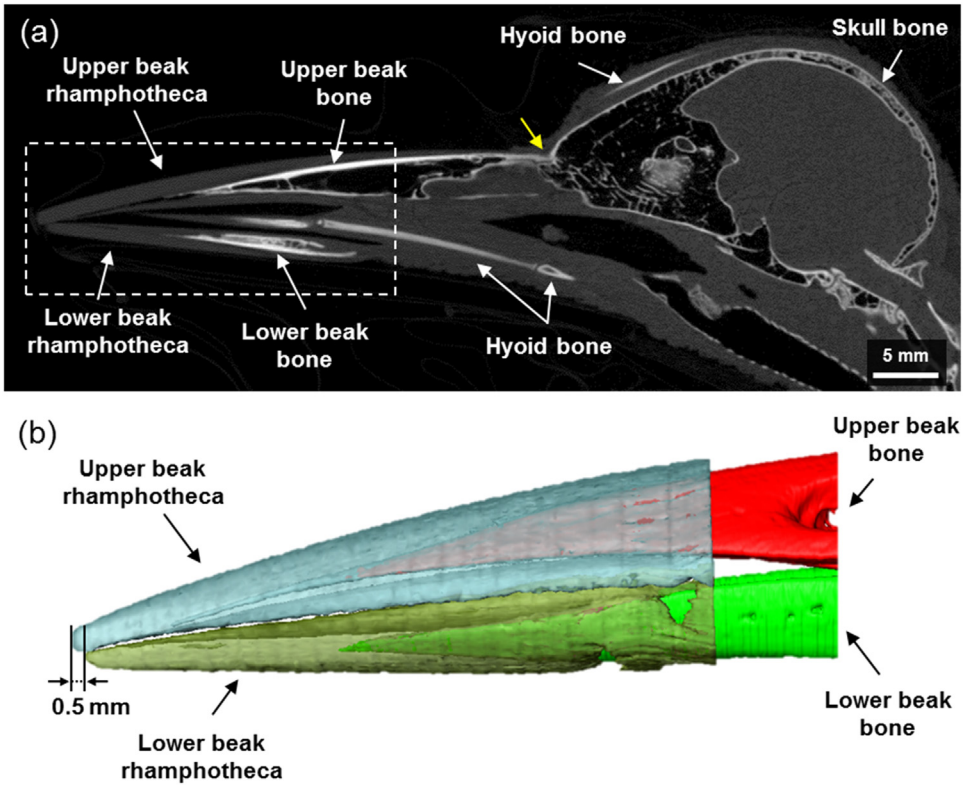

Fig. 1. Head anatomy of an acorn woodpecker (*Melanerpes formicivorus*) from micro-computed tomography. (a) Sagittal-section view and (b) a transparent three-dimensional reconstructed image of the upper and lower beaks (light blue: the upper beak rhamphotheca, yellow: the lower beak rhamphotheca, red: the upper beak bone, and green: the lower beak bone). (For interpretation of the references to color in this figure legend, the reader is referred to the web version of this article.)

(EDS) to characterize the microstructural features and chemical composition. Although the EDS analysis has some limitations based on its low spatial/volumetric accuracy compared to other surface characterization techniques (e.g., X-ray photoelectron spectroscopy or inductively coupled plasma with mass spectroscopy and/or atomic emission spectroscopy), it provides site-specific elemental composition at the micron scale, which cannot be obtained by the latter techniques. A typical X-ray interaction volume provided by EDS is on the order of a few cubic microns while the length scale of microstructures investigated in this manuscript ranged over at least 50–100 μm, and the accuracy of 1 μm as the spatial resolution is small enough. Regarding the energy resolution, another set of EDS data for the chicken and woodpecker skull bones were previously reported (i.e., Lee et al., 2014) by using the same technique.

To obtain accurate characterization data and remove artifacts generated by surface topology, an identical sample preparation procedure was used as in our previous study (Jung et al., 2016); Here, embedded samples in epoxy were cut into smaller pieces along the transverse cross-section (which exposes both rostral and caudal sides at the body center) and subsequently polished on one side initially using a set of SiC abrasive papers followed by a 50 nm alumina slurry.

2.4. Mechanical characterization by nanoindentation

Elastic moduli were acquired by nanoindentation (TI 950 TriboIndenter, Hysitron, Minneapolis, MN) with a diamond cube corner tip on polished transverse cross-sectional pieces of a chicken and an acorn woodpecker skull bone. Multiple indentations ($N = 10$ at each location) were carried out with displacement controlled indents to a maximum depth of a 500 nm. The detailed procedure is identical to our previous study (Jung et al., 2016). A paired sample t-test was used to compare statistically significant differences of the Young's moduli between the two different bone regions for each skull bone. The criterion for statistical significance was chosen as $p < 0.05$.

3. Results and discussion

3.1. Macroscale structure

The lateral view μ-CT image of the woodpecker head structure is presented in Fig. 1a. The upper and lower beaks of rhamphotheca are illustrated with a gray contrast while the upper and lower beak bones are visualized with a bright white contrast. This indicates the difference of X-ray intensities between the two materials. The hyoid bone and skull bones were observed with a white contrast. For a better visualization, a magnified and transparent 3D μ-CT image of the upper and lower beaks (shown in a white dot box in Fig. 1a, including both the rhamphotheca and bones) is reconstructed, as shown in Fig. 1b. The difference in length between the upper beak rhamphotheca (light blue) and the lower beak rhamphotheca (yellow) is 0.5 mm (shorter than the previous report by Wang et al., 2011a). The bones of the upper beak (red) and the lower beak (green) are also shown. The beak rhamphotheca sheath fully covers the upper and lower beak bones, and the upper beak bone is directly connected to the skull bone (as indicated by the yellow arrow, Fig. 1a). These two different materials/structures and the link between the upper beak bone and the skull bone are critical for initial energy dissipation with subsequent residual stress propagated to the skull bone.

Fig. 2 shows the anatomies of the skull bone structures for a chicken and an acorn woodpecker based on reconstructions from micro-computed tomography. Fig. 2a shows the structure of a domestic chicken including the upper and lower beak, frontal, parietal, and jugal bones. The color scale represents the gradation of mineral density (i.e., blue (low density) to red (high density)). In general, the lower beak bone of avian species is separated from other bones in the skull, it is only connected to the skull by ligament tissues, as described earlier (Bock, 1964). The mineral density distribution of the chicken skull bone is quite interesting: the upper and lower beak bones generally have a higher mineral density than the skull; however, the density of the parietal bone seems to be particularly dense, higher or similar to that of the upper and lower beak bones (as shown in Fig. 2a). Other skull bones

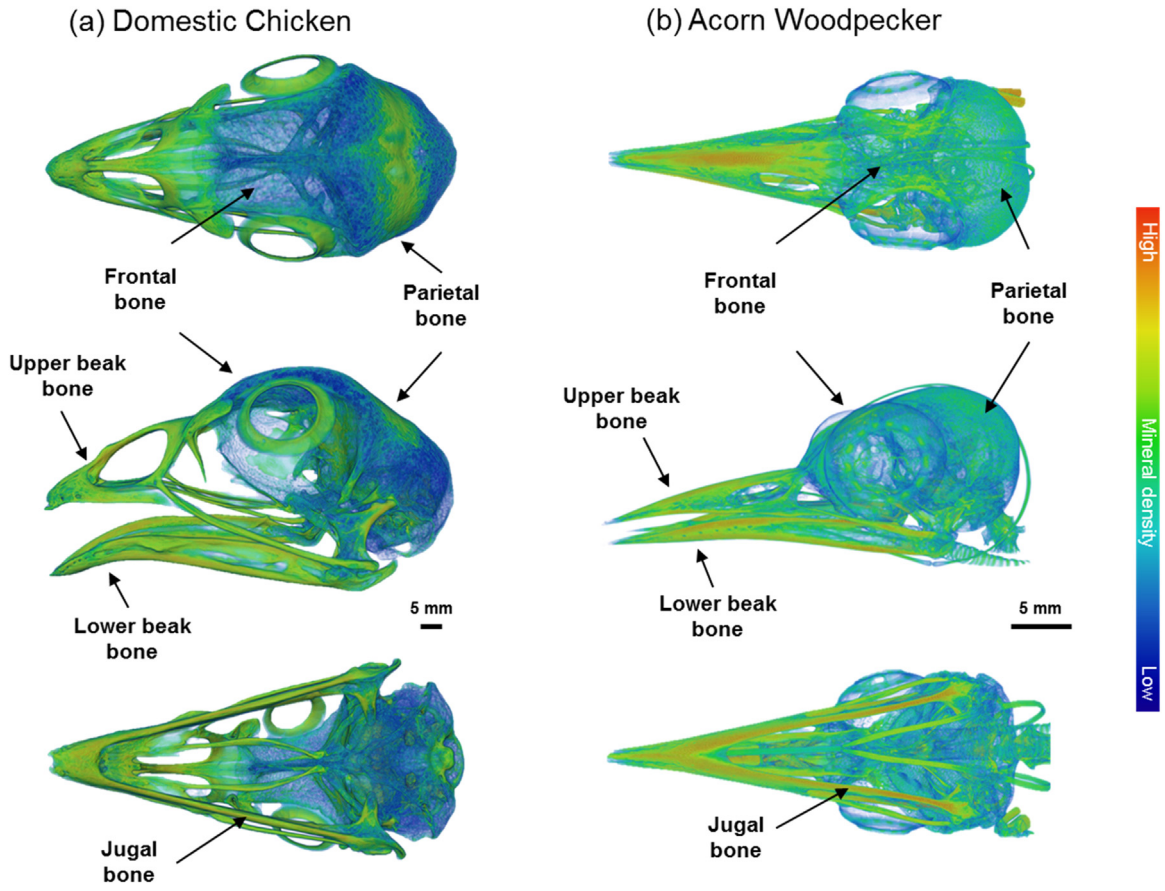

Fig. 2. Skull bone structures in (a) domestic chicken (*Gallus gallus*) adapted from (http://digimorph.org/) and (b) acorn woodpecker (*Melanerpes formicivorus*) adapted from (Jung et al., 2016). A dorsal (top), lateral (middle), and ventral (bottom) view reconstructed from micro-computed tomography. Note that X-ray intensity scale is not same between (a) and (b) because of the different scanning conditions, therefore, only a qualitative comparison in each species is possible.

(the entire frontal bone and some parts of the parietal bone) appear to have a lower density based on the μ-CT scan data. Because the X-ray intensity scale of Fig. 2a and 2b cannot be normalized due to the lack of use of a standardized material (i.e., imaging phantom) during scanning, only the relative comparison of mineral distribution between the two models is possible. From Fig. 2, we can estimate which regions may have more mineralized or denser regions, in advance, before selecting the ones that need to be investigated and cut as representative units. Using this insight from the CT-scans, we chose and measured mechanical properties at each selected region. Therefore, the different color distribution for each species (Fig. 2) is a good indication of different mechanical properties or structural properties as a non-destructive selection tool.

Generally, the anatomy of the woodpecker skull bone is rather similar to that of the chicken but the mineral density distribution is distinct from the chicken skull; the density is relatively homogeneous on the entire skull bone in the lateral view of μ-CT image (as shown in Fig. 2b, the dorsal view (the middle) image shows no color variation on the skull bone) and is much lower than the upper and lower beak bone densities, as reported by our previous study (Jung et al., 2016).

3.2. Microscale structure

Fig. 3 shows a comparison of transverse cross-sections of a chicken and an acorn woodpecker on the frontal and the parietal bones. In Fig. 3a, the frontal bone of the chicken presents a rounded T-shape for the cortical bone with a large portion of trabecular bone inside. The parietal bone shows bold lines of cortical bone at the edge, and a large portion of trabecular bone inside the cortical bone. Compared with the chicken frontal bone, the cross-sectional view of the woodpecker (Fig. 3b) has a sharp, triangular shape, and shows much smaller trabecular and cortical bone thicknesses. Table 1 summarizes the μ-CT analytical data for each skull bone. Gibson (Gibson, 2006) discussed the scaling effect since woodpeckers have smaller brains than humans, with the smaller brain being advantageous. The chicken showed a larger (76%) total volume of the skull bone (V_s) than the woodpecker. The ratio of the skull bone volume to the head volume (V_s/V_w) of the chicken was 42% larger (0.75) compared to the woodpecker (0.57), indicating that the skull bone volume might be minimized to reduce mass in the latter.

The average trabecular thickness (T_b) of the chicken frontal and parietal bone was larger than the woodpecker due to not only the general scaling effect but also to its lack of flight. The difference in T_b between the frontal and parietal bones is small for both species, indicating the trabecular structure remained: 1) as thin as possible close to minimize the weight even in the non-flying species, and 2) thick enough to support the surrounding cortical bones to act as a structural reinforcement. The average cortical thickness (T_c) shows that the chicken frontal and parietal bones are much thicker than the woodpecker; however, the ratio of the average cortical thickness to the whole head volume (T_c/V_w) of the woodpecker was 57 ~ 64% higher than the chicken. Compared to trabecular bone, cortical bone consists of a dense and highly mineralized material (i.e., an organic template of collagen mixed with hydroxyapatite, an inorganic mineral) with a multiscale hierarchical structure (i.e., osteon) (Meyers and Chen, 2014; McKittrick et al., 2010). Despite its high stiffness, it can also have a good toughness (energy dissipation) thanks to multiple crack-arresting mechanisms (Meyers et al., 2013; Meyers and Chen, 2014; Ritchie, 2011). This

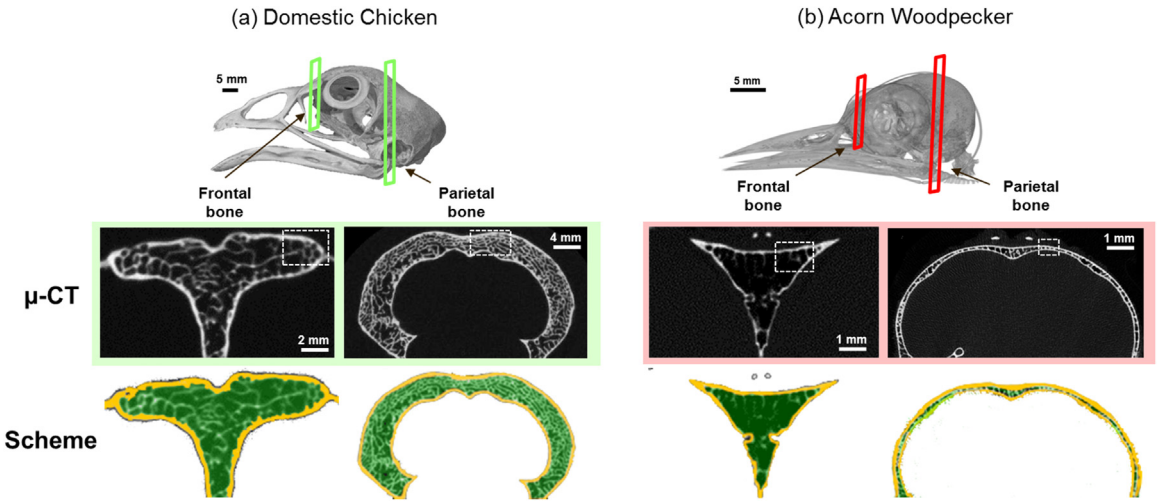

Fig. 3. A comparison of transverse-cross section view of the skull bone structures in (a) domestic chicken and (b) acorn woodpecker. The frontal bone (left) and the parietal bone (right). The bone morphometry quantification data is given in Table 1. The quantification was done at the indicated white rectangle regions on each image. In the scheme, yellow lines represent the region of cortical thickness calculation, while green area represents the region of trabecular thickness calculation. (For interpretation of the references to color in this figure legend, the reader is referred to the web version of this article.)

indicates that the woodpecker skull bones have relatively larger portions of cortical bone than the chicken, which might be helpful to prevent severe damage from impact, providing additional stiffness and energy dissipation.

A bone morphometric analysis was performed to calculate the closed porosity, the tissue volume (TV) and the bone volume (BV). The ratio of the bone volume and tissue volume (BV/TV) of the chicken is two times higher than that for the woodpecker. The calculated porosity varied for each bone, as shown in Table 1. The total porosity can be expressed by (Gibson and Ashby, 1999):

$$\frac{\rho_p}{\rho_d} = (1-\varphi) \tag{1}$$

where φ is a total porosity (volume fraction), ρ_p and ρ_d are the density of the porous and dense material, respectively. If the relative density (ρ_p/ρ_d) in the cellular structures is < 0.3, it can be considered as an open cell structure with the definition of the relative stiffness (or relative modulus) (Meyers and Chen, 2014):

$$\frac{E_p}{E_d} \approx \left(\frac{\rho_p}{\rho_d}\right)^n \tag{2}$$

where n is a power exponent ranging from 1 to 3 (related to the stiffness of the material; close to 1 for non-mineralized materials and 3 for highly mineralized materials), while E_p and E_d are the Young's moduli of the porous and dense material. If the relative density is > 0.3, it can be described as a closed-cell structure and the relative stiffness can be defined by the following equation (Gibson and Ashby, 1999)

$$\frac{E_p}{E_d} = \gamma^2\left(\frac{\rho_p}{\rho_d}\right)^n + \frac{(1-\gamma)\rho_p}{\rho_d} + \frac{P_0(1-2\nu_p)}{E_d\left(1-\frac{\rho_p}{\rho_d}\right)} \tag{3}$$

where γ is the fraction of solid in the closed cell edges, ν_p is the measured Poisson's ratio and P_0 is the gas pressure in the closed pores. The relative densities of the frontal and parietal bones of the chicken and woodpecker are measured following Eq. (1) and the results are summarized in Table 1. According to Eq. (1), the frontal bones of both species are considered as closed-cell, and therefore follow Eq. (3), while

Table 1
Two- and three- dimensional bone morphometry results in a chicken and woodpecker. Note that the brain weight is the median value of its average range taken from (Bennett and Harvey, 1985). The measured values were presented as the mean with a standard deviation (S.D.).

Parameter	Chicken		Woodpecker	
Location	Frontal bone	Parietal bone	Frontal bone	Parietal bone
Total volume of the skull bone in 3D model (V_s)	13,527 mm^3		3,230 mm^3	
Brain volume (V_b) in 3D, based on the density of the human brain (1,040 kg/m^3 (Oda et al., 2006))	4,567 mm^3 (or 4.75 g) (*Galliformes* (Bennett and Harvey, 1985))		2,403 mm^3 (or 2.5 g) (*Piciformes* (Bennett and Harvey, 1985))	
Whole head volume in 3D ($V_w = V_s + V_b$)	18,094 mm^3		5,633 mm^3	
Ratio of the skull bone volume to the whole head volume in 3D (V_s/V_w)	0.75		0.57	
Average trabecular thickness in 2D (T_b, μm) (S.D.)	95 (± 27)	82 (± 20)	51 (± 7)	54 (± 5)
Average cortical thickness in 2D (T_c, μm) (S.D.)	166 (± 5)	76 (± 3)	81 (± 2)	41 (± 1)
Ratio of the average cortical thickness to the whole head volume (T_c/V_w, x 10^{-5} mm^{-2})	0.92	0.42	1.43	0.73
Tissue volume (TV, x10^{12} μm^3)	8.73		3.60	
Bone volume (BV, x10^{12} μm^3)	2.50		0.52	
Bone volume / tissue volume (BV/TV, %)	28.6		14.4	
Closed porosity (%) in 3D	4.9	77.1	20.5	27.2
Open porosity (%) in 2D	57.5	3.0	61.3	87.5
Total porosity (%) in 2D	59.6	77.8	69.3	90.9
Relative density	0.404	0.222	0.307	0.091
Solid cell type (Gibson and Ashby, 1999)	Closed	Open	Closed	Open

the parietal bones of both species can be considered as open-cell and follow Eq. (2). According to Eq. (3), a higher closed porosity causes an increased relative modulus due to the cellular densification as a combination effect of cell-wall bending (resulting in enhanced cell-wall stiffness due to their connectivity) and cell-wall buckling/fracture (resulting in edge contraction and membrane stretching as well as enclosed gas pressure) (Gibson and Ashby, 1999; Ashby, 1983). This increased modulus can be applied to the chicken and woodpecker frontal bones; however, the closed porosity of the woodpecker frontal bone (~21%) is much higher than the chicken (~5%). Thus, the relative modulus of the woodpecker frontal bone is more affected by the amount of the closed pores than the chicken frontal bone because numerous enveloped chambers in the closed pores play a role as pressure vessels. In contrast, for the open-cell of the parietal bones, the degree of mineralization and the total (open) porosity are the only dominant variables to determine its relative stiffness because the relative modulus of the open cell is not affected by other variables (Gibson and Ashby, 1999), implying chemical composition as followed by the degree of mineralization plays more important role in the open-cell foam structure.

3.3. Microstructure and chemical composition

Zhu et al. (2014) reported that the Young's moduli of woodpecker skull bones ranged from 4 to 9 GPa and varied according to location. This is likely to be due to underlying chemical and structural differences in specific regions of the skull bone, involving different calcium contents or varying degrees of mineralization within each region. To confirm this, optical and scanning electron micrographs were used to show the bone structure in both chickens and woodpeckers (Fig. 4). For the chicken frontal bone, an optical micrograph in Fig. 4a shows the white colored trabecular bone inside. The upper right part of the image shows the cortical bone and the rectangle box indicates the area of higher magnification of a back-scattered scanning electron (BSE) micrograph. For the chicken parietal bone, an optical micrograph shows similar structure to the frontal bone but the higher magnification BSE image (white rectangle box area in the OM image) shows numerous small pores (~ 35 μm in diameter) in the trabecular network. These small pores corroborate the previous μ-CT results that the parietal bone of chickens shows the highest closed porosity. The frontal and parietal bone of the woodpecker show much fewer closed pore spaces, as shown Fig. 4b. An optical micrograph shows two circular, large spaces (dark contrast), which are surrounded by the cortical and trabecular bone (gray). It appears that closed pore spaces in 2D but the pores are categorized as open because of their connectivity in the 3D analysis. The higher magnification BSE micrograph also shows several larger and smaller circular spaces around the bones. Each cross-section shows the location where the EDS spectrum was acquired. EDS quantification shows differences in mineral content: calcium to phosphorus ratios (Ca/P ratio) of the chicken are 1.40 in the frontal bone and 1.45 in the parietal bone (Ca/P for hydroxyapatite is 1.67), whereas the Ca/P ratios of the woodpecker are higher: 1.69 in the frontal bone and 1.64 in the parietal bone. The semi-quantified values of nitrogen (N) contents, which usually come from organic materials, show relatively higher values (9–12 at%) in the chicken skull bone than in the woodpecker skull bone (7–11 at%). Conversely, larger gaps in both calcium (Ca, 14–16 at% in chickens and 23–27 at% in woodpeckers) and carbon content (C, 15–20 at% in woodpeckers and 27–32 at% in chickens) are found between the two species. The levels of oxygen (O, 32–36 at%) and phosphorus (P, 10–14 at%) content remain consistent overall. The presence of carbon is likely from either carbonated calcium phosphate or organic materials. Although the apatitic bones of mammals can be substituted with carbonate ions, it is minimal (Meyers and Chen, 2014). Thus, those higher C contents in chickens are more likely due to the higher content of organic materials (i.e., collagen type 1 or other proteins). This implies that the woodpecker skull bone has a higher Ca/P ratio and possibly higher stiffness, when compared to the chicken. The higher Ca/P in the woodpecker might affect the work of fracture and/or toughness; however, the correlation between the microstructure and chemical composition implies that there is a tradeoff: the chicken has a large difference in the amount of closed porosity between the frontal and parietal bone, while woodpeckers show similar level of closed porosity for both bones. To confirm this interpretation, the mechanical properties need to be evaluated at the same locations.

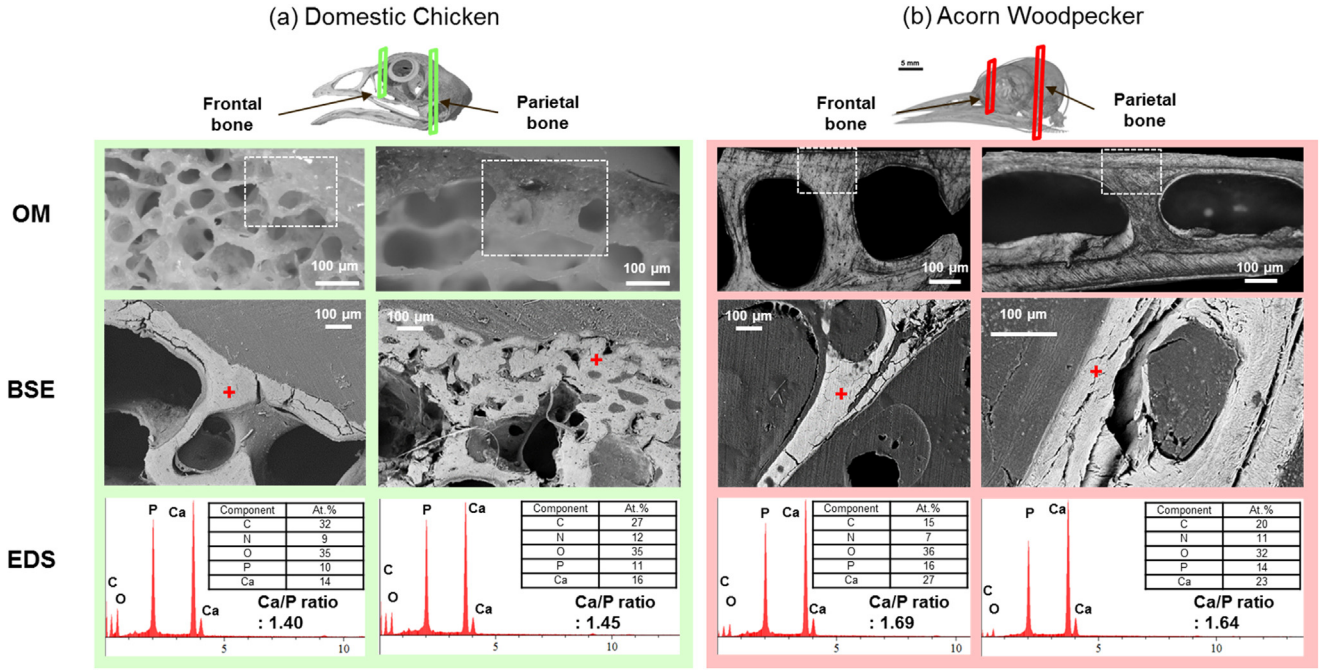

Fig. 4. Optical and back-scattered scanning electron micrographs of transverse-cross section view of the skull bone structure in (a) domestic chicken and (b) acorn woodpecker. The white rectangles represent the area of higher magnification micrographs of back-scattered scanning electron micrographs. The red cross-hairs represents where the energy-dispersive X-ray spectra were obtained and analyzed.

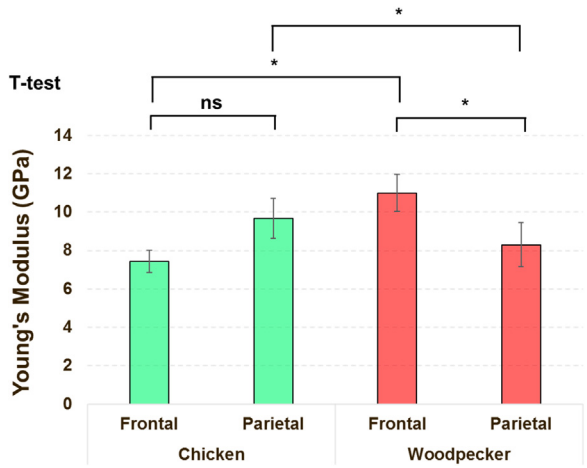

Fig. 5. Young's moduli from nanoindentation testing of the skull bone in domestic chicken (green) and acorn woodpecker (red). Comparisons where no statistically significant difference was observed are marked with an "ns" symbol. Otherwise, asterisk (*) symbols are marked when $p < 0.05$. (For interpretation of the references to color in this figure legend, the reader is referred to the web version of this article.)

3.4. Mechanical properties

As shown in Fig. 2, the discrepancy of the X-ray contrast of the skull bone between chickens and woodpeckers might imply a difference of the mechanical properties for each location. The Young's moduli of the transverse cross-sections of the chicken and the woodpecker skull bones were measured by a nanoindentation method; results are presented in Fig. 5. In the chicken, the frontal bone (7.3 GPa) has a slightly lower Young's modulus than the parietal bone (9.7 GPa) but this difference is not statistically significant ($p = 0.21$). The woodpecker has a higher modulus in the frontal bone (11.0 GPa) compared to the parietal bone (8.3 GPa) ($p < 0.002$). The frontal bone of the woodpecker has a higher Young's modulus than that of the chicken ($p < 0.020$) and the parietal bone of the chickens has a higher Young's modulus than that of the woodpecker ($p < 0.026$).

For the woodpecker, the higher modulus of the frontal bone, compared to parietal bone, might be due to a higher Ca/P ratio, which affects the density of the calcium phosphate mineral compounds (i.e., monobasic calcium phosphate monohydrate shows a 0.5 M ratio of Ca/P and a density of 2.22 g/cm^3, while a 1.67 of Ca/P ratio and a density of 3.155 g/cm^3 for hydroxyapatite) (Eliaz and Metoki, 2017). For the chicken, the parietal bone showed a higher Ca/P than the frontal bone, resulting in a higher elastic modulus. However, the measured elastic modulus is not statistically different; therefore, the effect of the mechanical property mismatch is not significant in the chicken skull bones. In contrast, the measured Young's moduli of the frontal bone of woodpeckers are statistically larger than the parietal bone; thus, indicating that the frontal bone of woodpeckers has adapted with a stiffer and thicker cortical bone, while the parietal bone shows a more compliant and thinner cortical bone. This mismatch of the Young's moduli between the frontal and parietal bones is beneficial to mitigate the propagated impact force/pressure through the skull bone.

4. Conclusions

This study provides structural, chemical, and mechanical properties towards understanding the impact-resistance of the woodpecker skull. The differences between the skull bones of a chicken and an acorn woodpecker were evaluated. Characterization of structural and chemical properties was performed using optical microscopy, scanning electron microscopy with energy dispersive X-ray spectroscopy, and micro-computed tomography. A bone morphometric analysis was carried out to obtain a relative size of the whole head and brain volume with its ratio, a tissue and bone volume and its ratio, and a closed porosity in the selected volume of interest. Mechanical properties of the frontal and parietal bone were obtained from nanoindentation in both species. The main findings are summarized in Fig. 6 and described as below:

- The general anatomy of the skull between the chicken and woodpecker is similar but the mineral density distribution is different: the

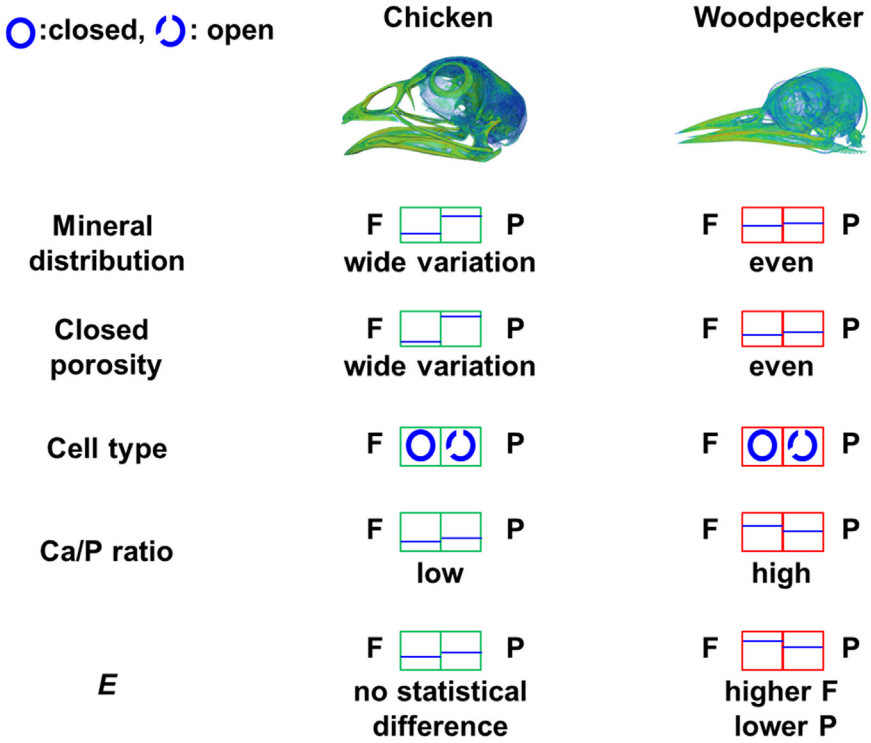

Fig. 6. Schematic diagram of the summarized main findings. Note that F and P are the frontal and parietal bone, respectively. *E* is the Young's modulus. Blue lines represent relative values of each bone. Blue circles represent the simplified shape of cell type; a closed circle for closed cell, an opened circle for an open cell. Green and red boxes represent the chicken and woodpecker skull bone, respectively. The relative values are rough visual estimations without the upper and lower ends. (For interpretation of the references to color in this figure legend, the reader is referred to the web version of this article.)

woodpecker shows an even distribution, while the chicken shows variation.

- Variations of mechanical/chemical/structural differences between the frontal and parietal bone are observed. Compared to the chicken, the woodpecker shows:
  - o a uniform level of closed porosity (20 ~ 27%), which affects the relative moduli mainly governed by the closed-cell foam structure,
  - o the same solid cell type: a closed-cell type in the frontal bone and an open-cell type in the parietal bone,
  - o a higher Ca/P ratio (1.64–1.69),
  - o a higher Young's modulus (8.3–11.0 GPa) than the ones determined for chicken (7.3–9.7 GPa), based on the experimental nanoindentation measurements.
- For the chicken, the mismatch of cell type between the frontal bone as a closed-cell and the parietal bone as an open-cell results in minimizing the relative modulus in both bones, implying the chicken is not as specialized as the woodpecker skull bone.
- These experimental findings will be useful for further dynamic mechanical simulation or mechanical analyses.

Acknowledgments

The authors thank to Ms. Esther Cory and Dr. Robert L. Sah for μ-CT scans. This work is supported by a Multi-University Research Initiative through the Air Force Office of Scientific Research (AFOSR-FA9550-15-1-0009) (J.J., D.K., J.M., S.E.N., N.Y., M.M., A.P.) and a National Science Foundation, Biomaterials Grant 1507978 (J.M.). Some of the work described here was carried out using shared research resources at the National Center for Microscopy and Imaging Research (NCMIR) at UCSD supported by the NIH under award number P41 GM103412 (M.H. Ellisman). The authors also would like to acknowledge the digimorph.org (Dr. Jessica A. Maisano) and NSF grant IIS-0208675 to T. Rowe (for woodpeckers) and NSF grant DBI-0743460 to B. Dumont (for chicken) for sharing the raw CT data. This work was performed in part at the San Diego Nanotechnology Infrastructure (SDNI) of UCSD, a member of the National Nanotechnology Coordinated Infrastructure, which is supported by the National Science Foundation (Grant ECCS-1542148).

References

Ashby, M.F., 1983. The mechanical properties of cellular solids. Metall. Trans. A 14, 1755–1769.
Bennett, P.M., Harvey, P.H., 1985. Brain size, development and metabolism in birds and mammals. J. Zool. 207, 491–509.
Bock, W.J., 1964. Kinetics of the avian skull. J. Morphol. 114, 1–41.
Bock, W.J., 1999. Functional and evolutionary morphology of woodpeckers. Ostrich 70, 23–31.
Bock W.J., Miller W.D., 1959. The scansorial foot of the woodpeckers, with comments on the evolution of perching and climbing feet in birds: American Museum of Natural History.
Bouxsein, M.L., Boyd, S.K., Christiansen, B.A., Guldberg, R.E., Jepsen, K.J., Müller, R., 2010. Guidelines for assessment of bone microstructure in rodents using micro–computed tomography. J. Bone Miner. Res. 25, 1468–1486.
Doube, M., Kłosowski, M.M., Arganda-Carreras, I., Cordelières, F.P., Dougherty, R.P., Jackson, J.S., Schmid, B., Hutchinson, J.R., Shefelbine, S.J., 2010. BoneJ: free and extensible bone image analysis in ImageJ. Bone 47, 1076–1079.
Eliaz, N., Metoki, N., 2017. Calcium phosphate bioceramics: a review of their history, structure, properties, coating technologies and biomedical applications. Materials 10, 334.
Gibson, L.J., 2006. Woodpecker pecking: how woodpeckers avoid brain injury. J. Zool. 270, 462–465.
Gibson, L.J., Ashby, M.F., 1999. Cellular Solids: Structure and Properties. Cambridge university press.
Homberger, D.G., Meyers, R.A., 1989. Morphology of the lingual apparatus of the domestic chicken, *Gallus gallus,* with special attention to the structure of the fasciae. Am. J. Anat. 186, 217–257.
http://digimorph.org/.
Jollie, M.T., 1957. The head skeleton of the chicken and remarks on the anatomy of this region in other birds. J. Morphol. 100, 389–436.
Jung, J.-Y., Naleway, S.E., Yaraghi, N.A., Herrera, S., Sherman, V.R., Bushong, E.A., Ellisman, M.H., Kisailus, D., McKittrick, J., 2016. Structural analysis of the tongue and hyoid apparatus in a woodpecker. Acta Biomater. 37, 1–13.
Lee, N., Horstemeyer, M.F., Rhee, H., Nabors, B., Liao, J., Williams, L.N., 2014. Hierarchical multiscale structure-property relationships of the red-bellied woodpecker (*Melanerpes carolinus*) beak. J. R. Soc. Interface 11, 20140274.
Liu, Y., Qiu, X., Zhang, X., Yu, T.X., 2015. Response of woodpecker's head during pecking process simulated by material point method. PLoS One 10, e0122677.
Marbury R., 2014. Taxidermy Art: A Rogue's Guide to the Work, the Culture, and How to Do It Yourself: Artisan.
May, P.A., Fuster, J., Newman, P., Hirschman, A., 1976. Woodpeckers and head injury. Lancet 307, 1347–1348.
May, P.A., Fuster, J.M., Haber, J., Hirschman, A., 1979. Woodpecker drilling behavior: an endorsement of the rotational theory of impact brain injury. Arch. Neurol. 36, 370–373.
McKittrick, J., Chen, P.-Y., Tombolato, L., Novitskaya, E., Trim, M., Hirata, G., Olevsky, E., Horstemeyer, M., Meyers, M., 2010. Energy absorbent natural materials and bioinspired design strategies: a review. Mater. Sci. Eng.: C. 30, 331–342.
Mehdizadeh, S.A., Neves, D.P., Tscharke, M., Nääs, I.A., Banhazi, T.M., 2015. Image analysis method to evaluate beak and head motion of broiler chickens during feeding. Comput. Electron. Agric. 114, 88–95.
Meyers, M.A., Chen, P.Y., 2014. Biological Materials Science: Biological Materials, Bioinspired Materials, and Biomaterials. Cambridge University Press.
Meyers, M.A., McKittrick, J., Chen, P.-Y., 2013. Structural biological materials: critical mechanics-materials connections. Science 339, 773–779.
Oda, J., Sakamoto, J., Sakano, K., 2006. Mechanical evaluation of the skeletal structure and tissue of the woodpecker and its shock absorbing system. JSME Int. J. Ser. A Solid Mech. Mater. Eng. 49, 390–396.
Odgaard, A., Gundersen, H.J.G., 1993. Quantification of connectivity in cancellous bone, with special emphasis on 3-D reconstructions. Bone 14, 173–182.
Parfitt, A.M., Drezner, M.K., Glorieux, F.H., Kanis, J.A., Malluche, H., Meunier, P.J., Ott, S.M., Recker, R.R., 1987. Bone histomorphometry: standardization of nomenclature, symbols, and units: report of the ASBMR histomorphometry nomenclature committee. J. Bone Miner. Res. 2, 595–610.
Ritchie, R.O., 2011. The conflicts between strength and toughness. Nat. Mater. 10, 817–822.
Tolman, C.W., 1967. The feeding behaviour of domestic chicks as a function of rate of Pecking By a surrogate companion. Behaviour 29, 57–62.
Van Den Heuvel, W.F., 1991. Kinetics of the skull in the chicken (Gallus Gallus domesticus). Neth. J. Zool. 42, 561–582.
Van Den Heuvel, W.F., Berkhoudt, H., 1997. Pecking in the chicken (Gallus Gallus Domesticus): motion analysis and stereotypy. Neth. J. Zool. 48, 273–303.
Wang, B., Yang, W., McKittrick, J., Meyers, M.A., 2016. Keratin: structure, mechanical properties, occurrence in biological organisms, and efforts at bioinspiration. Prog. Mater. Sci. 76, 229–318.
Wang L., Fan Y., 2013. Role of mechanical performance of cranial bone in impact protection of woodpecker brain–a finite element study. World Congress on Medical Physics and Biomedical Engineering, IFMBE Proceedings, 39, pp. 165–167.
Wang, L., Cheung, J.T.-M., Pu, F., Li, D., Zhang, M., Fan, Y., 2011a. Why do woodpeckers resist head impact injury: a biomechanical Investigation. PLoS One 6, e26490.
Wang, L., Zhang, H., Fan, Y., 2011b. Comparative study of the mechanical properties, micro-structure, and composition of the cranial and beak bones of the great spotted woodpecker and the lark bird. Sci. China Life Sci. 54, 1036–1041.
Wu, C.W., Zhu, Z.D., Zhang, W., 2015. How woodpecker avoids brain injury? J. Phys.: Conf. Ser. 628, 012007.
Yoon, S.-H., Park, S., 2011. A mechanical analysis of woodpecker drumming and its application to shock-absorbing systems. Bioinspiration Biomim. 6, 016003.
Zhou, P., Kong, X.Q., Wu, C.W., Chen, Z., 2009. The novel mechanical property of tongue of a woodpecker. J. Bionic Eng. 6, 214–218.
Zhu, Z., Wu, C., Zhang, W., 2014. Frequency Analysis and Anti-Shock Mechanism of Woodpecker's Head Structure. J. Bionic Eng. 11, 282–287.